Urokinase-targeted fusion by oncolytic sendai virus eradicates orthotopic glioblastomas by pronounced synergy with interferon-β gene

Hasegawa, Yuzo
Department of Neurological Surgery, Chiba University, Graduate School of Medicine | DNAVEC Corporation

Kinoh, Hiroaki
DNAVEC Corporation

Iwadate, Yasuo
Department of Pathology, Graduate School of Medical Sciences, Kyushu University

Onimaru, Mitsuho
Department of Pathology, Graduate School of Medical Sciences, Kyushu University

他

出版情報：Molecular Therapy. 18 (10), pp.1778-1786, 2010-10. Nature Publishing Group
バージョン：

MTHE-D-09-00590R3 (revised manuscript)

Title:

Urokinase-targeted fusion by oncolytic Sendai virus eradicates orthotopic glioblastomas by pronounced synergy with interferon-β gene

Authors:
Yuzo Hasegawa[1], Hiroaki Kinoh[6], Yasuo Iwadate[2], Mitsuho Onimaru[2], Yasuji Ueda[6], Yui Harada[3], Satoru Saito[3], Aki Furuya[3], Takashi Saegusa[4], Yosuke Morodomi[3,5], Mamoru Hasegawa[6], Shigeyoshi Saito[7], Ichiro Aoki[7], Naokatsu Saeki[1], and Yoshikazu Yonemitsu[3]

Affiliations:
[1]Department of Neurological Surgery, Chiba University Graduate School of Medicine, Chiba, Japan
[2]Department of Pathology, Graduate School of Medical Sciences, Kyushu University, Fukuoka 812-8582, Japan
[3]R&D Laboratory for Innovative Biotherapeutics, Graduate School of Pharmaceutical Sciences, Kyushu University, Fukuoka 812-8582, Japan
[4]Department of Neurological Surgery, Chiba Rosai Hospital, Chiba, Japan
[5]Department of Surgery and Science, Graduate School of Medical Sciences, Kyushu University, Fukuoka 812-8582, Japan
[6]DNAVEC Corporation, Tsukuba, Ibaraki 305-0856, Japan
[7]Molecular Imaging Research Center, National Institute of Radiation Therapy, Chiba, Japan

Short Running Head: ***Fusogenic oncolysis of GM by targeting uPA***

Correspondence to: Yoshikazu Yonemitsu, M.D., Ph.D.
R&D Laboratory for Innovative Biotherapeutics,
Graduate School of Pharmaceutical Sciences, Kyushu University
Rm 505 Collaborative Research Station II
3-1-1 Maidashi, Higashi-ku
Fukuoka 812-8582, Japan
Phone/Fax: +81-92-642-4777
E-mail: yonemitu@med.kyushu-u.ac.jp

Disclosures:
Dr. Yonemitsu is a member of the Scientific Advisory Board of DNAVEC Corporation.

Key Words: recombinant Sendai virus, urokinase-type plasminogen activator, glioblastoma multiforme, interferon-β

Abstract

Glioblastoma multiforme (GM), the most frequent primary malignant brain tumor, is highly invasive due to the expression of proteases, including urokinase-type plasminogen activator (uPA). We here show the potential of our new and powerful recombinant Sendai virus (rSeV) showing uPA-specific cell-to-cell fusion activity (rSeV/dMFct14 (uPA2), named "BioKnife") for GM treatment, an effect that was synergistically enhanced by arming BioKnife with the interferon-β (IFN-β) gene. BioKnife killed human GM cell lines efficiently in a uPA-dependent fashion, and this killing was abolished by PA inhibitor-1. Rat gliosarcoma 9L cells expressing both uPA and its functional receptor uPAR (9L-L/R) exhibited high uPA activity on the cellular surface and were highly susceptible to BioKnife. Although parent 9L cells (9L-P) were resistant to BioKnife and to BioKnife expressing IFN-β (BioKnife-IFNβ), cell-cell fusion of 9L-L/R strongly facilitated the expression of IFN-β, and in turn, IFN-β significantly accelerated the fusion activity of BioKnife. A similar synergy was seen in a rat orthotopic brain GM model with 9L-L/R *in vivo*; therefore, these results suggest that BioKnife-IFNβ may have significant potential to improve the survival of GM patients in a clinical setting.

(183 words)

Introduction

Glioblastoma multiforme (GM), the most frequent primary malignant brain tumor, is highly invasive and intractable, and the median survival of patients bearing GM is merely 1 year with the current standard treatments, including surgery and radiotherapy.[1] A recent clinical trial revealed that temozoromide, an oral alkylating agent, achieved significant improvement of the median survival of patients of GM to 14.6 months[2]; however, another study reported that 73.5% of patients still die within less than 2 years and 72.2% experience recurrence.[3] The highly invasive nature of GM is a cause of great frustration among surgeons and is responsible for the high rate of local recurrence; extended resection for complete removal of tumor cells is usually difficult without injuring surrounding brain tissues, and therefore, the surgical margin is frequently regarded as positive.

There is thus an urgent need for new approaches in GM treatment. Virus-based therapeutics for glioblastoma have been evaluated in clinical studies over the last decade, including a packaging cell-mediated local production of retroviruses expressing herpes simplex virus thymidine kinase (HSV-tk).[4] Even though these viruses have been shown to increase oncolytic activity and tumor specificity, no significant therapeutic effects have been reported in the clinical trials to date[5]; therefore, researchers are focusing their current efforts on improving new viruses that target GM[6-9] including a unique oncolytic adenovirus that targets mutant variant III of the epithelial growth factor receptor (EGFRvIII), which is a glioblastoma-specific mutant. In our effort to achieve an efficient virus-based therapeutics, we previously demonstrated a cancer

vaccine regimen combined with intratumor injection of F/M-gene-deleted nontransmissible recombinant Sendai virus (rSeV) expressing the interleukin-2 (IL-2) gene in a rat orthotopic model.[10] This was the first experimental protocol to successfully eliminate an established rat 9L gliosarcoma in the brain, and suggested that rSeV would be safe and useful for the clinical practice of glioblastoma therapy. However, because of the highly malignant nature of the 9L tumor, the tumor elimination ratio was modest (-30%) even by this regimen, and there is thus need of a more powerful tool before moving to clinical study.

In order to develop a new therapeutic modality, we returned to the current understanding of the molecular mechanisms involved in the invasive nature of GM, and have recently focused on the protease system. It has been reported that GM frequently expresses urokinase-type plasminogen activator (uPA) and that its invasiveness is closely related to uPA activity.[11] uPA can be activated by a high affinity receptor, uPAR, on the cell surface, after which uPA activates matrix metalloproteases (MMPs) and plasmin, resulting in the degradation of extracellular matrix. Also, activation of these uPA-related proteins induces several intracellular signaling pathways via growth factor receptors, thereby facilitating cell adhesion, migration and proliferation. A number of reports have demonstrated the close relationship between increased levels of local uPA and poor prognosis in cancer patients, including patients bearing GM.[12] Since uPA activity is specifically upregulated in cancerous tissue but not in normal tissue, and uPA activity is observed on the cancer cell surface, it seems reasonable that a therapeutic modality targeting uPA could selectively kill cancer cells without significant damage to

the surrounding normal tissue.

To realize this concept, we recently developed novel oncolytic viruses based on a type of rSeV that selectively shows MMP- or uPA-specific cell killing activity via cell-cell fusion,[13,14] namely, "oncolytic rSeV." These new viruses were developed by several major genetic modifications: 1) deletion of the gene encoding matrix (M) protein, which resulted in the loss of budding of secondary viral particles and accumulation of HN (hemagglutinin/neuraminidase) and F (fusion) proteins on the cell surface; 2) replacement of trypsin-susceptible amino acid sequences of the F-gene with targeted protease-specific ones; and 3) truncation of the cytoplasmic domain of the F-gene. As a result, our recent study demonstrated that uPA-targeted oncolytic rSeV (rSeV/dMFct14(uPA2): named "BioKnife") showed optimal performance and was applicable to various types of human malignancies.[14]

Therefore, we here examined the therapeutic potential of BioKnife for treating human glioma and a rat orthotopic model of highly malignant 9L gliosarcoma. Our results indicate that BioKnife may be useful for GM treatment. In addition, we revealed that BioKnife armed with the interferon-β (IFN-β) gene exhibited pronounced killing of GM *in vitro* and *in vivo*.

Results

uPA activity-specific cell fusion and killing using BioKnife in human GM cells

In the initial stage of this study, we tested our hypothesis, namely, that uPA activity-dependent cell fusion/killing could be accomplished using infection of the BioKnife vector into five independent lines of human GM cells (U87, U138, U251, U373, and A172) and into a rat 9L gliosarcoma. As shown in Fig. 1A, a catalytic uPA activity assay revealed that 3 (U138, U251, and U373) of the 6 cell lines expressed a significant amount of active uPA in culture media. To assess the cytotoxic activity of BioKnife (rSeV/dMFct14(uPA2)) on these cells, a WST assay was performed. As expected, BioKnife expressing GFP (BioKnife-GFP) efficiently killed GM cells that expressed high levels of uPA (U373 and U251) (Fig. 1B, left panels and two graphs). Since modest cytotoxicity due to the M-gene-deleted control recombinant virus (rSeV/dM-GFP, see Supplementary Figure S1) was found in U138, A172, and 9L cells, no significant increase in the cytotoxic effect of BioKnife-GFP was detected in these cells. Addition of a sufficient amount of PAI-1, a specific inhibitor for uPA, into the culture medium of U251 cells completely abolished the BioKnife-dependent cytotoxicity (right graph), confirming the uPA-specific killing of U251 cells.

Second, we assessed the time course of the cytotoxicity of BioKnife-GFP and the infection efficiencies based on the rSeV-dM-GFP-positive cell ratio determined by FACS analyses on these 5 human GM cell lines and the rat gliosarcoma cell line 9L. As shown in Supplementary Figure S2, even when a small amount of viruses was used

(MOI=1.25), the 5 human cell lines were relatively susceptible to rSeV/dM infection, usually showing an rSeV-dM-GFP-positive cell ratio of over 70%; however, significant and strong cell death was seen only in the cell lines U251 and U373 (see Figure 1B for representative results). 9L cells, in contrast, were highly resistant both to rSeV/dM infection and BioKnife-mediated cell death. Together with the data shown in Figure 1, these results suggest that uPA activity may predict the cytotoxic activity of BioKnife-GFP, and that the infection efficiency is not always important for BioKnife-mediated cell death.

Next, we focused on U251 cells, which was the only of the human GM cell lines tested that could develop subcutaneous xenograft tumors on immune deficient mice (data not shown). Also, the effect of BioKnife expressing the human IFN-β gene (hIFN-β) was examined, because hIFN-β has been proven effective for the treatment of experimental and clinical glioma.[15,16] As shown in Fig. 2A, recombinant human IFN-β protein (rhIFN-β) demonstrated a dose-dependent cytotoxic effect on U251, with over 75% cytotoxicity at 10,000 U/mL (equivalent to 256 ng/ml). A direct comparison study revealed that BioKnife-hIFNβ had a significantly greater cell-killing effect on U251 than any of the other viruses tested (all $P<0.01$) (Fig. 2B). When U251 cells were implanted on the subcutis of the right flank of *nu/nu* mice, however, the superiority of the antitumor effect of BioKnife-hIFNβ was not apparent, because all the therapies tested were sufficiently effective in this model (Fig. 2C).

uPA activity on the cellular surface is critical for optimal BioKnife activity

To clarify whether BioKnife shows significant synergism with IFN-β *in vitro* and *in vivo*, we generated 9L cells that were less susceptible to both BioKnife (Fig. 1B) and recombinant murine IFN-β protein (rmIFN-β) (Fig. 4A) and that stably expressed murine uPA and/or murine uPAR. As shown in Fig. 3A, Western blot analyses confirmed that the levels of uPA and uPAR were undetectable in the parent 9L (9L-P), and that the transfected gene-specific protein synthesis had occurred (9L-C: 9L with control plasmid; 9L-L: 9L with uPA ligand cDNA; 9L-R: 9L with uPA receptor cDNA; and 9L-L/R: 9L with both uPA ligand cDNA and uPA receptor cDNA). Interestingly, only 9L-L/R cells expressed high uPA activity in both the culture medium and on the cell surface, while 9L-L cells synthesized uPA only in the culture medium, suggesting that a high level of uPAR expression is required to accumulate active uPA on the cell surface (Fig. 3B). In contrast, expression of the uPA-specific endogenous inhibitor PAI-1 was almost undetectable on the cell surface of all cells tested, and was significantly downregulated in the culture media of 9L-L/R and 9L-L cells ($P<0.01$), suggesting a negative feedback mechanism of uPA or catalytic degradation of PAI-1 by uPA (Fig. 3C).

Using these cells, we next tested the biological action of BioKnife. As shown in Fig. 3D, BioKnife-GFP showed optimized cytotoxicity on 9L-L/R cells (Fig. 3D, graph; $P<0.01$). Interestingly, Hoechst 33342 staining (middle two panels) revealed that 9L-L/R cells forming a syncytium contained both living cells strongly expressing the GFP transgene (green, upper two panels, arrowheads) and dying cells stained by PI (red, lower two panels, arrowheads).

Taken together, these findings indicate that BioKnife shows its optimized biological action—namely, the killing of tumor cells via induction of syncytium formation—when there is a sufficient amount of uPA activity on the cell surface.

Pronounced synergy of BioKnife and the IFN-β transgene for killing of 9L-L/R cells *in vitro*

Next, we examined the synergy between BioKnife and IFN-β for GM therapy using 9L-L/R cells. We here used the murine IFN-β gene and recombinant protein (mIFN-β and rmIFN-β), because the species-specificity of IFN-β between rodents and humans is widely known. Because our preliminary study showed that the 9L-L/R cell killing activity of BioKnife expressing the mIFN-β gene (BioKnife-mIFNβ) was superior to that of BioKnife-GFP at 3 days after virus inoculation (data not shown; representative data are seen in Fig. 4D), we first examined the susceptibility of 9L-L/R cells to BioKnife-mIFNβ.

Recombinant mIFN-β protein (rmIFN-β) showed significant cytotoxicity to 203G murine glioma cells in a dose-dependent manner; however, 9L-L/R cells were highly resistant to rmIFN-β, even when a huge amount of rmIFN-β (~10% of cytotoxicity at 120,000 U/mL, equivalent to 3,077 ng/ml) was used (Fig. 4A). In addition, inoculation of the conventional non-transmissible vector rSeV/dF-mIFNβ or BioKnife-mIFNβ to parent 9L cells that were resistant to BioKnife-mediated cell fusion produced a similar amount of mIFN-β protein in a dose-dependent manner (Fig. 4B, left graph). In contrast, we were surprised to observe that the infection of BioKnife-sensitive 9L-L/R cells with

BioKnife-mIFNβ dramatically enhanced mIFN-β expression (over 2-logs higher than the expression levels obtained using the others) (Fig. 4B, right graph), indicating that cell fusion markedly accelerated the expression of the transgene.

To seek the possible mechanism underlying the enhanced expression of the mIFN-β transgene, we next assessed the time course of the genome copy numbers of viruses by quantitative real-time RT-PCR targeting the N gene. In the case of the Sendai virus, it is well known that genome replication reflects its transcription well. As shown in Fig. 4C, cell fusion via BioKnife potentiates the number of viral genome copies on 9L-L/R (susceptive to cell fusion, right graph), but not on 9L-P (resistant to cell fusion, left graph). Interestingly, strong and early amplification of genome copies of BioKnife-GFP was found in 9L-L/R cells, and declined 3 days after infection. In contrast, a delayed and sustained increase of genome copies was found when using BioKnife-mIFNβ. It was suggested, therefore, that this sustained increase of genome copies and its transcription might have resulted in the enhanced IFN-β transgene expression shown in Fig. 4B.

Next, we questioned the reverse effect—in other words, whether mIFN-β might accelerate cell fusion and killing even in mIFN-β-insensitive 9L-L/R cells. To examine this hypothesis, we checked the cytotoxicity over a time course. Interestingly, the cytotoxicity induced by BioKnife-GFP peaked on days 4 to 5, while cells treated with BioKnife-mIFNβ already demonstrated a nearly peak cell death on day 3 (Fig. 4D). Then we asked whether the transgene expression of mIFN-β might accelerate the cell fusion/killing and whether rmIFN-β might have an effect similar to that seen using the

transgene. As shown in Fig. 4E, a pronounced acceleration of cytotoxicity on 9L-L/R was observed when using BioKnife-mIFNβ. In contrast, a modest enhancement of cell killing by BioKnife-GFP was seen under a higher concentration of rmIFN-β on day 4, indicating the drastic improvement in the biological activity of BioKnife conferred by transgene expression of the mIFN-β gene.

Pronounced synergy of BioKnife and the IFN-β transgene for killing of 9L-L/R cells *in vivo*

Prior to the *in vivo* study assessing the therapeutic potentials of BioKnife, we investigated the effect of forced uPA/uPAR gene expression on the growth and behavior of 9L cells *in vitro* and *in vivo.* As shown in Fig. 5A, the growth activity of 9L-L/R *in vitro* was identical to those of 9L-P and 9L-C. In contrast, the *in vitro* wound-healing assay revealed the significantly enhanced migratory activity of 9L-L/R cells (Fig. 5B). Magnetic resonance imaging (MRI) also demonstrated that the local growth of 9L-L/R tumors in the rat brain *in vivo* was roughly identical to that seen with 9L-P tumors (Fig. 5C; 9L-P: n=12 animals; 9L-L/R: n=15 animals); however, five animals that received 9L-L/R cells showed the invasive growth of tumors to the hippocampus and/or corpus callosum, as well as the tumor dissemination to the fourth ventricle packing and/or nodule formation at the distant central nervous system (Fig. 5D), indicating that forced expression of uPA/uPAR resulted in the increased malignant potential of 9L tumors.

Pronounced synergy of BioKnife and the IFN-β transgene for killing of 9L-L/R

cells *in vivo*

Finally, the therapeutic potential of BioKnife-mIFNβ on an orthotopic rat model of GM was investigated using 9L-L/R cells. We first assessed the expression level of transgene mIFN-β *in vivo* in 9L-L/R tumor-bearing rat brain tissue. Two days after injection of vector at $1x10^7$ ciu/dose, the brain tissue was subjected to specific ELISA. As shown in Fig. 6A, strong enhancement of transgene expression was found when using BioKnife-mIFNβ as compared to that seen using rSeV/dF-mIFNβ at the ipsilateral site, and the findings were similar to those seen in the *in vitro* experiment (Fig. 4B).

The therapeutic benefit on the survival of tumor bearing rats is shown in Fig. 6B; all control rats that were treated with PBS or non-fusogenic rSeV/dM-GFP were dead within 46 or 52 days after tumor inoculation, respectively. Gene transfer of mIFN-β via rSeV/dF significantly improved the survival of rats with IFN-β-insensitive 9L-L/R ($P<0.05$), suggesting that this therapeutic effect might have been due to the well-known immune-mediated antitumor effect of IFN-β, but not due to its direct cytotoxicity on tumor cells. Similarly, the survival of tumor-bearing rats that received BioKnife-GFP was also significantly prolonged compared to those in the PBS or rSeV/dM-GFP group ($P<0.05$, respectively). Compared to these efficacies, BioKnife-mIFNβ showed a dramatic enhancement of the therapeutic potential of BioKnife: namely, no dead animals were observed during the trial. These surviving rats exhibited no residual tumor cells in their brain tissue either macroscopically or microscopically (data not shown).

These results provided clear evidence of a pronounced synergistic effect between

the fusogenic activity of BioKnife and the IFN-β transgene *in vitro* and *in vivo*.

Discussion

We here investigated the potential and mechanism of our recently developed uPA-targeted oncolytic virus, BioKnife, to treat a rat model of GM. Key observations obtained in this study were as follows: 1) among 9L cells that were stably transformed with the uPA and/or uPAR gene, accumulation of uPA activity on the cellular surface was crucial for the optimal biological functioning of BioKnife; 2) there was a dramatic synergy between cell fusion/cytotoxicity and IFN-β transgene expression via BioKnife—namely, we observed an acceleration of cell fusion and a dramatic increase of transgene expression; and 3) the synergistic effects of BioKnife-IFNβ were effective for treating a rat orthotopic brain tumor model with 9L-L/R, even if the tumor itself was resistant to IFN-β therapy alone. These findings indicate the potential utility of BioKnife expressing the IFN-β gene and provide important information related to the biological parameters predicting the efficacy of BioKnife in future clinical trials.

During the course of the current study, we had some unexpected findings; however, some of these anomalies were resolved in subsequent experiments. First, the expression level of uPA did not always predict the cytotoxic activity of BioKnife (e.g., U138, Fig. 1), and this question was resolved by an experiment using 9L, which showed that the cell surface accumulation of uPA, but not its release, was critical for the biological activity of BioKnife (Fig. 3). To the best of our knowledge, this is the first demonstration that the expression of uPAR is critical for facilitating the accumulation of active uPA on the cell surface. Second, although BioKnife-GFP appeared to be capable of facilitating syncytium formation of U138 and U172 (Fig. 1B. panels), the observed

cytotoxicity did not always support the notion that such syncytium formation occurred (Fig.1B, graph). This contradictory data could be explained by the data of Fig. 3D: namely, syncytium formation did not always correlate with dying cells, at least at this time point.

Next, we should discuss why PAI-1 expression in the culture media from 9L-L/R and 9L-L was downregulated, since it was previously shown that uPA enhances the expression of PAI-1.[20] A possible explanation of this paradox is that the uPA/PAI-1 complex may mask epitopes recognized by the ELISA system, because RT-PCR analysis could not detect a significant reduction of PAI-1 mRNA in these cells (data not shown).

A most important question remains—namely, by what mechanism is the dramatic synergy between BioKnife and the IFN-β transgene realized? It has been widely accepted based on previous studies[21,22] that type-I IFNs inhibit cell-cell fusion and viral replication of paramyxoviruses, including Sendai virus. However, our data obtained by recombinant viruses suggest that this rule may not apply in all situations; for example, the recombinant virus yield during the amplification process of BioKnife encoding IFN-β using LLC-MK2 cells is significantly increased more than several-fold compared with that of BioKnife expressing other transgenes (unpublished data). Interestingly, the cell-cell fusion of epithelial and dendritic cells induced by measles virus, a member of *paramyxoviridae*, was shown to be enhanced by type-I IFNs,[23] suggesting that acceleration of the cell-cell fusion induced by IFN-β might be cell- and/or species-specific. In the present study, we also found that BioKnife-mediated cell-cell

fusion strongly enhanced IFN-β transgene expression, which reached over 2-logs higher than that seen when using non-fusogenic virus. Since the transgene of BioKnife was expressed by its own viral expression machinery, these findings theoretically indicate that cell-cell fusion facilitates viral protein synthesis; however, to the best of our knowledge, there has been no published data that could explain these findings. Therefore, further studies will be needed to investigate the molecular mechanisms of such synergies.

Finally, since *in vivo* experiments using the orthotopic GM model in this study demonstrated a dramatic therapeutic effect, the clinical relevance of our BioKnife-IFNβ should be discussed. First, almost all surgical specimens of GM were shown to express a high level not only of biologically active uPA but also uPAR,[24,25] suggesting that a majority of GM patients would be good candidates for this therapeutics. The current model may be clinically relevant to residual and disseminated tumor cells rather than solid tumors, because virus injection was started 1 day after tumor inoculation; therefore, the adjuvant use of BioKnife-IFNβ after mass reduction via, for example, surgery and/or stereotactic radiotherapy would be reasonable. Although it may be possible that such a protease-targeting strategy would show limited efficacy, because urokinase is variably expressed at different sites in the parenchyma of growing tumors, these theoretical considerations based on this study warrant further investigations and encouraged us to move this system to the clinic.

In conclusion, we here demonstrated the efficient control of a rat orthotopic model of GM via the marked synergistic actions of IFN-β gene transfer and BioKnife,

an oncolytic rSeV targeting uPA. These findings support the therapeutic potential of BioKnife-IFNβ for intractable GM in a clinical setting.

Materials and Methods

Cells, reagents, ELISA, plasmid vectors

The human brain tumor cell lines (U87, U138, U251, U373, and A172) and the rat cell line 9L were purchased from American Type Culture Collection (ATCC, Rockville, MD) or the European Collection of Cell Cultures (ECACC, England, UK). These cell lines were maintained in complete medium (RPMI 1640 for 203G and DMEM for the others) supplemented with 10% FBS, penicillin, streptomycin and 1% sodium pyruvate (Flow Laboratories, Mclean, VA) under a humidified atmosphere containing 5% CO2 at 37°C. ELISA was performed using commercially available kits for rat PAI-1 (Hyphen Biomed, Andresy, France) and for mIFN-β (PBL Biomedical Laboratories, Piscataway, NJ). Full-length murine uPA and uPAR cDNAs were cloned from total RNA of Lewis lung cancer cells (ATCC: CRL-1642) by RT-PCR, and human uPA and uPAR cDNAs were cloned from total RNA of human prostate tumor cells: PC3 (ATCC: CRL-1435) by RT-PCR. The sequences of PCR primers with *Bam HI* and *Nhe I* sites were the following: murine uPA, forward 5'-TCTAGCTAGCCGCCATGAAAGTCTGGCTGG CGAGC-3'/reverse 5'-CCGCGGATCCTCAGAAGGCCAGACCTTTCTC-3'; murine uPAR, forward 5'-TCTAGCTAGCCGCCATGGGACTCCCAAGGCGGCTG-3'/ reverse 5'-CCGCGGATCCTCAGGTCCAGAGGAGGACGCC-3'). Amplified cDNA fragments were digested with *Bam HI* and *Nhe I* and inserted into a pcDNA3.1 vector (Invitrogen, Carlsbad, CA). The full sequences of cDNAs were determined by direct sequencing.

Construction and recovery of BioKnife vectors

rSeVs and rSeV armed with IFN-β were constructed as described previously,[13,14,17] and all schematic structures of viruses used in this study were demonstrated in the Supplementary Figure S1. In brief, the parent plasmid pSeV18+/dM-GFP, in which the GFP had been substituted for the deleted M gene,[18] was digested with *Sal I* and *Nhe I*, and the F gene fragment (9,634 bp) was subcloned into LITMUS 38 (New England Biolabs, Beverly, MA). Site-directed mutagenesis was performed using a Quick-Change Mutagenesis Kit (Stratagene, La Jolla, CA), and the mutated F gene was returned to the pSeV18+/dF-GFP backbone. Murine and human IFN-β cDNA were previously cloned[19] and were inserted into the pSeV+18/Fct14(uPA2)dM-GFP plasmid. Recovery and amplification of the SeV vector were performed essentially as described before. Briefly, LLC-MK2 cells were transfected with a plasmid mixture containing each plasmid - pSeV+18/Fct14 (uPA2)dM-GFP, pGEM-NP, pGEM-P, and pGEM-L - in 110 µl of Superfect reagent (Qiagen, Tokyo, Japan). The transfected cells were maintained for 3 h, washed three times and incubated for 60 h in MEM containing araC. The cells were collected and lysed by three cycles of freezing and thawing. The lysate solution was incubated on the F/M-expressing LLC-MK2 cells in a 24-well plate. Twenty-four hours later, the cells were washed and incubated in MEM containing araC and 7.5 µg/ml trypsin plus 10 ng/ml urokinase (Cosmobio, Tokyo, Japan). The virus yield was expressed in cell infection units (CIU), as previously described.[13,14] Expression of murine or human IFN-β was determined by specific ELISA.

Virus titration

The virus titers were expressed as cell infectious units (CIU), which were estimated by infecting confluent LLC-MK2 cells in a 6-well plate with diluted solution as previously described.[13,14] In brief, LLC-MK2 cells were inoculated in duplicate with a series of dilutions of virus, then incubated for 1 hr and washed twice with PBS. Two days after infection, cells were fixed in methanol, incubated with anti-SeV primary antibodies, and then incubated with FITC-labeled goat anti-rabbit IgG(H+L) (Invitrogen, Carlsbad, CA). Immunofluorescent-positive cell were counted and cell infection units (CIU) per ml were calculated.

uPA activity assay and ELISA for PAI-1 and mIFN-β

Cells ($1.5x10^4$) in 60 μl medium were seeded in a 96-well dish, and the supernatants were collected after 48 h. The uPA activity or PAI-1 expression in the culture medium and on the cell surface of denucleated cells that were washed three times with a sufficient amount of PBS was measured using a colorimetric uPA Activity Assay Kit (Chemicon International, Temecula, CA) or ELISA kit for rat PAI-1, according to the manufacturer's instruction.

Cytotoxicity assay

Cells ($5x10^3$) were seeded in a 96-well dish with 100 μl medium containing various concentrations of recombinant hIFN-β (PBL Biomedical Laboratories), mIFN-β

(Chemicon International) proteins, or various amounts of viruses. At each time point, cytotoxicity was measured using a Premix WST-1 Cell Proliferation Assay System (Takara Bio Inc, Otsu, Shiga, Japan). Defining the cell viability of a negative control well as 100%, the cytotoxicity of each well was calculated by subtracting the corresponding viability from 100%.

uPA- and/or uPAR-expressing stable transfectants of 9L

9L Cells ($3x10^5$) were seeded in 6-well dishes with 2 ml medium/well, and the following day, the plasmid vectors were transfected using TransIT-LT1 Reagent (Mirus Bio Corporation, Madison, WI) according to the manufacturer's instructions. Gene-transferred 9L cells (9L-P: parent 9L; 9L-C: 9L with control plasmid; 9L-L: 9L with uPA ligand cDNA; 9L-R: 9L with uPA receptor cDNA; and 9L-L/R: 9L with both uPA ligand cDNA and uPA receptor cDNA) were maintained under 200 μg/ml of antibiotic G-418, and the clones surviving from single cells were selected twice.

Western blotting

Samples were lysed in lysis buffer containing 50 mM Tris HCL (pH 6.8) and 10% sodium dodecyl sulfate (SDS), and the protein concentration for each sample was determined by using a Bio-Rad Protein Assay kit (Bio-Rad Laboratories, Inc., Hercules, CA). Anti-mouse uPA (ab20789, rabbit, 1:1000; Abcam, Cambridge, UK), anti-mouse uPAR (AF534, goat; 1:1000; R&D Systems, Abingdon, UK), and anti-GAPDH (IMG-5143A, rabbit, 1:1000; IMGENEX Inc., San Diego, CA) were used as primary

antibodies. The secondary antibodies, anti-rabbit IgG (65-6120, goat, 1:10000; Invitrogen) or anti-goat IgG (561-71271, rabbit, 1:10000; Jackson ImmunoResearch Laboratories, West Grove, PA), were applied for 30 min. Specific bands were visualized using an ECL Plus Western Blotting Detection System (GE Healthcare, Little Charfont, UK).

Quantitative real-time RT-PCR assessing rSeV genome copies

Total cellular RNA was extracted from cultured cells with an ISOGEN system (Wako Pure Chemicals, Tokyo, Japan) according to the manufacturer's instructions, then treated with RNase-free DNAase I (Boehringer Mannheim, Mannheim, Germany). Twenty-five ng of total RNA was subjected to real-time RT-PCR. Real-time monitoring of the amplification and quantification of genome copies of rSeV were done using a model 7000 Sequence Detection System (Applied Biosystems, Ltd., Tokyo, Japan) by the TaqMan method according to the manufacturer's instructions. The oligonucleotide sequences of PCR primers and TaqMan probes targeting the N gene (Forward: 5'-CAATGCCGACATCGACCTAGA-3'; Reverse: 5'- CGTGCCCATCTTTCACCACTA -3'; TaqMan Probe: FAM-ACAAAAGCCCATGCGGACCAGGAC-TAMRA), a common sequence for all vector constructs used in this study, were purchased from Applied Biosystems. Three independent experiments were performed and the obtained data were statistically analyzed. The genome copies were standardized by the GAPDH level in each sample, and expressed as a relative fold increase compared with the control level.

Wound-healing assay

A single linear wound was made with a 200 μl pipette tip in confluent cultures of 9L-P or 9L-L/R cells and washed gently with PBS to remove cellular debris. The cells were transferred to fresh medium and incubated at 37°C. After 8, 16, and 24 hours, the cells were photographed and the area of each wound was calculated.

Animals

Female 7- to 8-week-old Balb/c *nu/nu* mice and male Fisher 344 rats were obtained from the Shizuoka Laboratory Animal Center. Animals were kept under specific pathogen-free and humane conditions in the animal care facility of Chiba University's Inohana campus. The animal experiments were reviewed and approved by the Institutional Animal Care and Use Committee and by the Biosafety Committee for Recombinant DNA experiments of Chiba University. These experiments were also done in accordance with the recommendations for the proper care and use of laboratory animals and according to The Law (No. 105) and Notification (No. 6) of the Japanese Government.

1. Subcutaneous tumor model of human U251 cells in nu/nu mice

1×10^7 U251 cells in 50 μl PBS plus 50 μl Matrigel (BD Biosciences, Bedford, MA) were subcutaneously injected into the right flank of nude mice. The tumor volume was calculated every 3 or 4 days, until day 28 after tumor inoculation, using the following

formula: volume = $a^2b/2$, where *a* is the shortest diameter and *b* is the longest. When the subcutaneous tumors grew over 200 mm^3 (defined as Day 0, usually 14 days after tumor inoculation), the mice were divided into treatment or control groups, and 100 μl PBS with or without each vector ($1x10^7$ CIU/dose) was injected 3 times (Day 0, 3, and 6) intratumorally using a 26-gauge needle.

2. Orthotopic GM model of 9L-L/R cells in rats

5×10^5 9L-L/R cells with 10 μl PBS were injected into rat brains using a microinjector (Harvard Apparatus, South Natick, MA) over 5 min, as previously described.[10] Briefly, rats were anesthetized with 50 mg/kg pentobarbital and placed in a stereotactic apparatus. A burr hole was made at an appropriate location (1 mm posterior to the bregma and 3 mm right to the midline). A 25-gauge needle was inserted at a point 3 mm ventral from the dura. On days 1, 4, and 7 after tumor injection, each SeV vector ($2x10^7$ CIU) with 20 μl PBS was injected in the same way. In addition, to evaluate the invasive activity of 9L-L/R, 1×105 of 9L-P or 9L-L/R cells with 10 μl PBS were injected into other rat brain in the same way and examined every 7 days with MRI. The invasive activity was measured at 4 weeks after tumor inoculation. The rats were observed daily until severe paresis, ataxia periophthalmic encrustations, or more than 20% weight loss developed.

Magnetic resonance imaging (MRI)

All rats were anaesthetized with 2.0% isoflurane (Abbott Japan, Tokyo, Japan) and

injected with 0.4 ml of Gd-DTPA (Magnevist, 0.002 ml/g, 50 mM, Bayer) intravenously 15 minutes before MRI measurement. All MRI experiments were performed on a 7.0-T MRI scanner (Magnet: Kobelco and JASTEC, Kobe, Japan; Console: Bruker Biospin, Ettlingen, Germany) with a volume coil for transmission (Bruker Biospin) and 2-ch phased array coil for reception (Rapid Biomedical, Rimpar, Germany). Multi-slice T_1-weighted MR images covering the entire brain (T1WI; multi-slice spin echo (SE), TR/TE = 400/9.57 ms, slice thickness = 1.0 mm, slice gap = 0, number of slices = 16, matrix = 256 × 256, field of view = 25.6 × 25.6 mm^2, average = 4) were acquired. The slice orientation was transaxial for all scans. Two independent neurosurgeons evaluated the MRIs to determine whether either "invasion" or "dissemination" were present. "Invasion" was defined as direct progression along neural fiber tracts and "dissemination" was defined as distant tumor growth separated from the original injection site by cerebrospinal fluid. When either invasion or dissemination was clearly observed in the transaxial plane, images in the horizontal and sagittal planes were also acquired. Image reconstruction and analysis were performed using ParaVision (Bruker Biospin).

Statistical analysis

All data were expressed as the means ± SD. The data were examined statistically using one-way ANOVA with Scheffe adjustment. When the number of evaluated groups was small, the data were subjected to the Kruskal-Wallis or the Mann-Whitney U test. The survival curves were determined using the Kaplan-Meier's method. The log-rank test

was used for comparison. A probability value of $P<0.05$ was considered statistically significant. Statistical analyses were determined using StatView software.

Acknowledgments

The authors thank Drs. Akihiro Tagawa, Takumi Kanaya, Hiroshi Ban, and Takashi Hironaka for their excellent technical assistance in vector construction and large-scale production. KN International Ltd. assisted in the revision of the language in this manuscript.

Funding

This work was supported in part by a grant from the Japanese Ministry of Education, Culture, Sports, Science, and Technology (to YY).

References

1. DeAngelis, LM (2001) Brain tumors. *N Engl J Med* **344**:114-123.

2. Stupp, R, Mason, WP, van den Bent, MJ, Weller, M, Fisher, B, Taphoorn, MJ, *et al.* (2005) Radiotherapy plus concomitant and adjuvant temozolomide for glioblastoma. *N Engl J Med* **352**:987-996.

3. Brandes, AA, Tosoni, A, Franceschi, E, Reni, M, Gatta, G, Vecht, C *et al.* (2009) Recurrence pattern after temozolomide concomitant with and adjuvant to radiotherapy in newly diagnosed patients with glioblastoma: correlation With MGMT promoter methylation status. *J Clin Oncol* **27**:1275-1279.

4. Rainov, NG, Jacobs, A, Quinones, A, Woiciechowsky, C, Sena-Esteves, M, Rainov, NG *et al.* (2000) A phase III clinical evaluation of herpes simplex virus type 1 thymidine kinase and ganciclovir gene therapy as an adjuvant to surgical resection and radiation in adults with previously untreated glioblastoma multiforme. *Hum Gene Ther* **11**:2389-2401.

5. Liu, TC, Galanis, E and Kirn, D (2007) Clinical trial results with oncolytic virotherapy: a century of promise, a decade of progress. *Nat Clin Pract Oncol* **4**: 101-117.

6. Yokoyama, T, Iwado, E, Kondo, Y, Aoki, H, Hayashi, Y, Georgescu, MM *et al.* (2008) Autophagy-inducing agents augment the antitumor effect of telerase-selve oncolytic adenovirus OBP-405 on glioblastoma cells. *Gene Ther* **15**:1233-1239.

7. Wakimoto, H, Kesari, S, Farrell, CJ, Curry, WT, Jr, Zaupa, C, Aghi, M *et al.* (2009) Human glioblastoma-derived cancer stem cells: establishment of invasive glioma models and treatment with oncolytic herpes simplex virus vectors. *Cancer Res* **69**:3472-481.

8. Liu, C, Sarkaria, JN, Petell, CA, Paraskevakou, G, Zollman, PJ, Schroeder, M *et al.* (2007) Combination of measles virus virotherapy and radiation therapy has synergistic activity in the treatment of glioblastoma multiforme. *Clin Cancer Res* **13**:7155-7165.

9. Piao, Y, Jiang, H, Alemany, R, Krasnykh, V, Marini, FC, Xu, J, Alonso, MM *et al.* (2009) Oncolytic adenovirus retargeted to Delta-EGFR induces selective antiglioma activity. *Cancer Gene Ther* **16**:256-265.

10. Iwadate, Y, Inoue, M, Saegusa, T, Tokusumi, Y, Kinoh, H, Hasegawa, M *et al.* (2005) Recombinant Sendai virus vector induces complete remission of established brain tumors through efficient interleukin-2 gene transfer in vaccinated rats. *Clin Cancer Res* **11**:3821-3827.

11. Rao, JS (2003) Molecular mechanisms of glioma invasiveness: the role of proteases. *Nat Rev Cancer* **3**:489-501.

12. Zhang, X, Fei, Z, Bu, X, Zhen, H, Zhang, Z, Gu, J *et al.* (2000) Expression and significance of urokinase type plasminogen activator gene in human brain gliomas. *J Surg Oncol* **74**:90-94.

13. Kinoh, H, Inoue, M, Washizawa, K, Yamamoto, T, Fujikawa, S, Tokusumi, Y *et al.* (2004) Generation of a recombinant Sendai virus that is selectively activated and lyses human tumor cells expressing matrix metalloproteinases. *Gene Ther* **11**:1137-1145.

14. Kinoh, H, Inoue, M, Komaru, A, Ueda, Y, Hasegawa, M and Yonemitsu, Y (2009) Generation of optimized and urokinase-targeted oncolytic Sendai virus vectors applicable for various human malignancies. *Gene Ther* **16**:392-403.

15. Mizuno, M and Yoshida, J (1998) Effect of human interferon beta gene transfer upon human glioma, transplanted into nude mouse brain, involves induced natural killer cells. *Cancer Immunol Immunother.* **47**:227-232.

16. Colman, H, Berkey, BA, Maor, MH, Groves, MD, Schultz ,CJ, Vermeulen, S *et al*. (2006) Radiation Therapy Oncology Group. Phase II Radiation Therapy Oncology Group trial of conventional radiation therapy followed by treatment with recombinant interferon-beta for supratentorial glioblastoma: results of RTOG 9710. *Int J Radiat Oncol Biol Phys.* **66**:818-824.

17. Li, HO, Zhu, YF, Asakawa, M, Kuma, H, Hirata, T, Ueda, Y *et al*. (2000) A cytoplasmic RNA vector derived from nontransmissible Sendai virus with efficient gene transfer and expression. *J Virol* **74**:6564-6569.

18. Inoue, M, Tokusumi, Y, Ban, H, Kanaya, T, Shirakura, M, Tokusumi, T *et al* (2003). A new Sendai virus vector deficient in the matrix gene does not form virus particles and shows extensive cell-to-cell spreading. *J Virol* **77**: 6419-6429.

19. Shibata, S, Okano, S, Yonemitsu, Y, Onimaru, M, Sata, S, Nagata-Takeshita, H *et al*. (2006) Induction of efficient antitumor immunity using dendritic cells activated by Sendai virus and its modulation of exogenous interferon-β gene. *J Immunol* **177**:3564-3576.

20. Shetty, S, Bdeir, K, Cines, DB and Idell, S (2003) Induction of plasminogen activator inhibitor-1 by urokinase in lung epithelial cells. *J Biol Chem*. **278**:18124-18131.

21. Tomita, Y and Kuwata, T (1981) Suppressive effects of interferon on cell fusion by Sendai virus. J *Gen Virol.* **55**:289-295.

22. Chatterjee, S, Cheung, HC and Hunter, E (1982) Interferon inhibits Sendai virus-induced cell fusion: an effect on cell membrane fluidity. *Proc Natl Acad Sci USA*. **79**:835-839.

23. Herschke, F, Plumet, S, Duhen, T, Azocar, O, Druelle, J, Laine, D *et al*. (2007) Cell-cell fusion induced by measles virus amplifies the type I interferon response. *J Virol.* **81**:12859-12871.

24. Yamamoto, M, Sawaya, R, Mohanam, S, Rao, VH, Bruner, JM, Nicolson, GL *et al*. (1994) Expression and localization of urokinase-type plasminogen activator receptor in human gliomas. *Cancer Res.* **54**:5016–5020.

25. Landau, BJ, Kwaan, HC, Verrusio, EN and Brem, SS (1999) Elevated levels of urokinase-type plasminogen activator and plasminogen activator inhibitor type-1 in malignant human brain tumors. *Cancer Res* **54**:1105-1108.

Legends for Figures

Figure 1.

Expression of uPA by human and rat brain tumor cells and their susceptibility to uPA-targeted rSeV/dMFct14(uPA2), namely, BioKnife. *P<0.01.

A. Expression of uPA by human GM cells (U87, U138, U251, U373, and A172) and rat gliosarcoma (9L) in culture medium. Four days after changing to fresh medium, the culture supernatant was subjected to a colorimetric catalytic assay. n=6 wells/group.

B. Susceptibility of brain tumor cells to BioKnife-GFP or control vector (rSeV/dM-GFP) at an MOI of 1.25. Four days after virus inoculation, cells were observed under a fluorescent microscope (panels) and the culture supernatant was subjected to cytotoxicity assay (graphs). In the case of U251, a group with PAI-1, a specific inhibitor of uPA, was included. Note that syncytium formation was observed in wells with U138, U251, U373, or A172 cells (panels), but not in wells with U87 or 9L cells. Significant cytotoxicity was observed against U251 and U373 cells, but not against A172 cells (left graph). Addition of PAI-1 almost completely abolished the BioKnife-dependent cytotoxicity (right graph). n=6 wells/group.

Figure 2.

Sole or combined effect of hIFN-β and BioKnife on U251 cells *in vitro* and *in vivo*.

*P<0.01 and $^{\#}P$<0.05.

A. Dose-dependent cytotoxic effect of rhIFN-β protein on U251 cells. Four days after addition of various amounts of rhIFN-β, the culture supernatant was subjected to

cytotoxicity assay. n=4 wells /group.

B. Cytotoxicity due to BioKnife-GFP (rSeV/dM-GFP as a control) and BioKnife-hIFNβ (rSeV/dF-GFP as a control). Four days after exposure of cells to viruses at an MOI of 0.3125 or 1.25, the culture supernatant was subjected to a cytotoxicity assay. n=6 wells/group.

C. Antitumor effect of BioKnife-GFP and BioKnife-hIFNβ on U251 tumor cells subcutaneously implanted into the right flank of nude mice. When the subcutaneous tumors grew over 200 mm^3 (defined as Day 0, usually 14 days after tumor inoculation), 100 μl PBS with or without each vector ($1x10^7$ CIU/dose) was injected 3 times (Day 0, 3, and 6) intratumorally using a 26-gauge needle. The data indicate the tumor volumes on day 28 after tumor inoculation.

Figure 3.

Accumulation of uPA on the cell surface is critical for the biological action of BioKnife.

*P<0.01

A. Representative Western blot analyses confirming the protein synthesis stably transfected with murine uPA and/or uPAR cDNA (9L-P: parent 9L; 9L-C: 9L with control plasmid; 9L-L: 9L with uPA ligand cDNA; 9L-R: 9L with uPA receptor cDNA; and 9L-L/R: 9L with both). Three independent experiments were performed and showed similar results.

B. Expression of uPA activity in the culture medium and on the cell surface from each

transfectant ($5x10^5$ cells). Forty-eight hours after cell seeding, the supernatant was subjected to the colorimetric uPA activity assay. Both 9L-L/R and 9L-L expressed a high level of uPA in the culture media; however, significant accumulation of uPA activity on the cell surface was seen only in 9L-L/R cells.

C. Expression of PAI-1 in the culture medium and on the cell surface from each transfectant. The supernatant obtained in B was subjected to ELISA for PAI-1.

D. Biological activity of BioKnife-GFP forming syncytium (panels, MOI=1.25) and leading cells to death (graph, MOI=1.25 and 5.0) on 9L-P or 9L-L/R cells (4 days after virus inoculation).

Panels) Demonstration of typical fluorescent microscopic findings detecting living cells (expressing foreign GFP genes) and dying cells (positive for PI). Nuclear staining was done using Hoechst 33342. No syncytium formation was found in parent 9L cells (9L-P, three left-hand panels). Note that GFP-expressing multinuclear cells (arrowheads) were negative for PI, and inversely, PI-positive dying cells (arrows) were negative for GFP (three right-hand panels). Two independent experiments were performed and showed similar results. The bar indicates 100 μm.

Graph) Cytotoxic assay for each transfectant. Only 9L-L/R cells demonstrated a significant increase of susceptibility to BioKnife-GFP. n=6/group.

Figure 4

Drastic synergy induced by BioKnife and mIFN-β gene transfer for killing 9L-L/R cells. **P*<0.01

A. Direct cytotoxic effect of recombinant murine IFN-β (rmIFN-β) on mouse glioma 203G and 9L-L/R cells. Four days after treatment with various amounts of rmIFN-β, a cytotoxicity assay was performed. Note that 203G cells were susceptible to the rmIFN-β protein and dose-dependent cytotoxicity was observed, while 9L-L/R cells were highly resistant to rmIFN-β protein even at a concentration of over 90,000 U/mL (equivalent to 2,308 ng/mL). Each group contains n=4.

B. Cell fusion via BioKnife enhances its mIFN-β transgene expression on 9L-L/R (susceptible to cell fusion, right graph), but not on 9L-P (resistant to cell fusion, left graph). Four days after exposure to each virus at each MOI, the mIFN-β protein level was measured by specific ELISA. No significant difference in expression levels was found between rSeV/dF-mIFNβ (non-fusogenic) and BioKnife-mIFNβ (fusogenic) using 9L-P cells (left graph). Note that over 2-logs higher mIFN-β protein levels were found with BioKnife-mIFNβ than with rSeV/dF-mIFNβ at any MOI in 9L-L/R cells (right graph). Significant, but very low levels of mIFN-β protein were detected when using rSeV/dM-GFP and BioKnife-GFP. Each group contains n=4.

C. Cell fusion via BioKnife potentiates viral genome copies on 9L-L/R (susceptible to cell fusion, right graph), but not on 9L-P (resistant to cell fusion, left graph). After exposure to each virus at an MOI of 1.25 on each time point, viral genome copies were quantified by real-time RT-PCR targeting of the N gene, their common sequence. Each data point was standardized by simultaneous amplification of GAPDH (the genome copies/GAPDH on day 1 in 9L-P cells treated with rSeV/dM-GFP= 1). Strong and early amplification of genome copies of BioKnife-GFP was found in 9L-L/R cells, and

declined 3 days after infection. In contrast, delayed and sustained increase of genome copies was found when using BioKnife-mIFNβ. Each group contains n=3.

D. Arming with the mIFN-β gene accelerates the cytotoxicity of BioKnife to mIFN-β-insensitive 9L-L/R cells. At various time points after exposure to each virus at an MOI of 1.25, a cytotoxicity assay was performed. Note that BioKnife-GFP showed peak cytotoxicity from day 4, while BioKnife-mIFNβ had already reached its peak cytotoxicity on day 3. Each group contains n=6.

E. Acceleration of cell fusion and cytotoxicity due to BioKnife is efficiently induced by mIFN-β gene transfer, but not by rmIFN-β protein. At various time points after exposure to each virus at an MOI of 1.25, a cytotoxicity assay was performed. Note that a modest but significant acceleration of cytotoxicity via BioKnife-GFP was found only in the presence of a high concentration of rmIFN-β (10,000U/mL) on day 4.

Figure 5.

Overexpression of uPA/uPA facilitates the invasive potential of 9L gliosarcoma cells.

A. Growth curve of 9L-L/R cell *in vitro*. No significant difference was found between 9L-P and 9L-C.

B. Wound-healing assay of 9L-P and 9L-L/R cells for assessing cell migration activity *in vitro*. A single linear wound was made with a 200 μl pipette, and each wound area was calculated 8, 16, and 24 hours later. Left panels are the representative phase-contrast images. Facilitated wound repair was found in 9L-L/R cells, indicating

that the overexpression of uPA/uPA accelerates cell migration activity.

C and D. Time course of the growth and invasiveness of 9L-P (n=12 animals) or 9L-L/R (n=15 animals) cells in rat brains assessed by sequential assessment with MR imaging. (C) All rats inoculated with 9L-P cells and 10 rats inoculated with 9L-L/R cells showed local growth around the injection site with neither detectable invasion nor dissemination. (D) A typical MR image showing invasion and dissemination. Five rats receiving 9L-L/R cells showed invasive cell transfer that included: 1) direct progression along neural fibers of the hippocampus and/or corpus callosum; 2) cerebrospinal fluid dissemination surrounding the cerebral ventricle and/or forming nodules on the brain surface.

Figure 6.

Impact of BioKnife expressing the mIFN-β gene for the treatment of an orthotopic rat brain tumor model with 9L-L/R. $*P<0.01$ and $^{\#}P<0.05$.

B. mIFN-β expression in ipsilateral (tumor bearing) and contralateral (no tumor) brain tissues 2 days after a single intratumor injection of BioKnife-mIFNβ or control vectors (rSeV/dM and rSeV/dF-mIFNβ) ($1x10^7$ ciu/dose). Each group contains n=8 animals.

C. Therapeutic effect of BioKnife-mIFNβ on an orthotopic rat brain tumor model. On days 1, 4, and 7 after tumor injection, each virus ($2x10^7$ CIU) in 20 μl PBS was injected, and the cell survival was observed. The data are the sum of two independent experiments.

Figure 1.

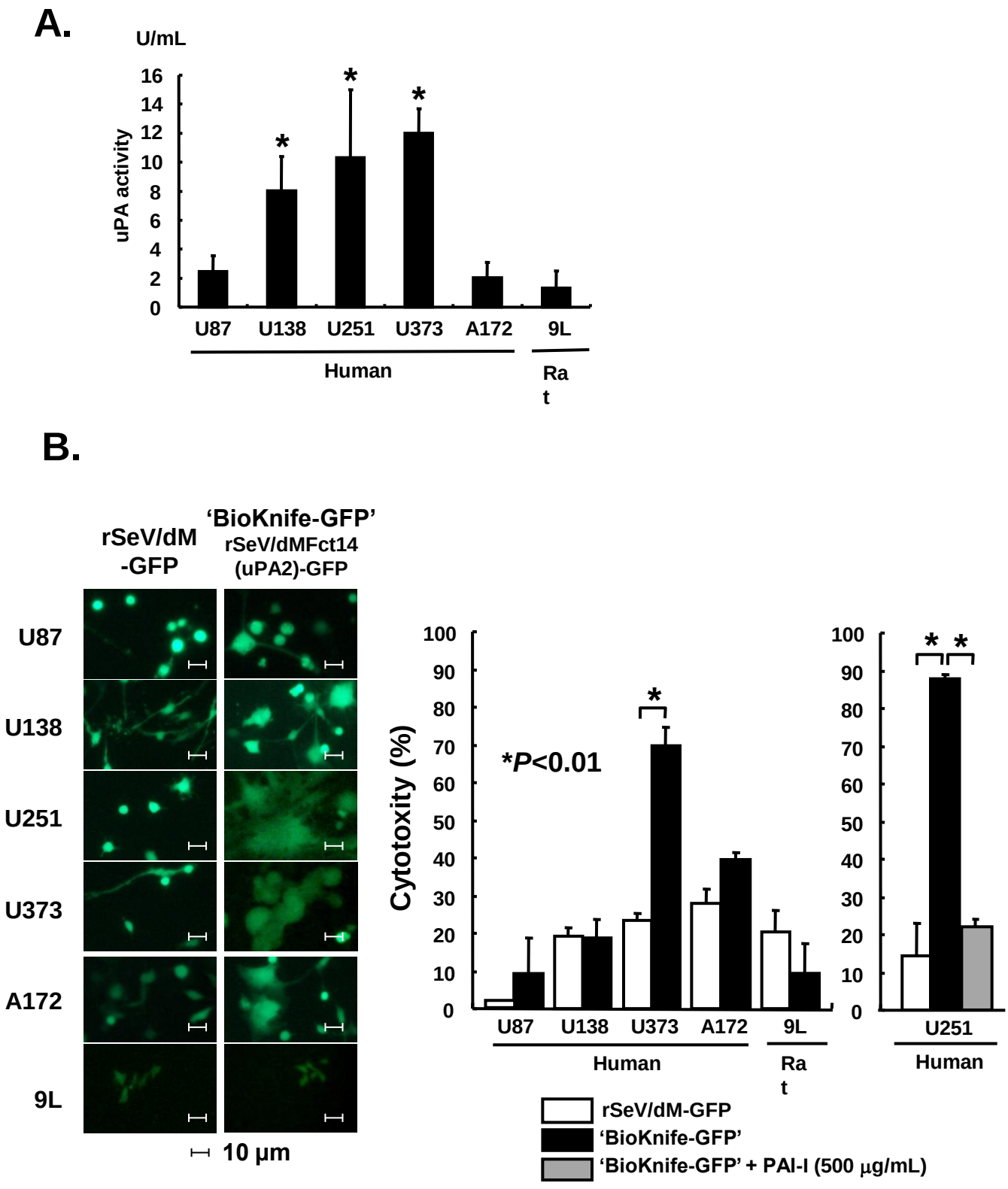
A.
U/mL
uPA activity
16
14
12
10
8
6
4
2
0
*
*
*
U87
U138
U251
U373
A172
9L
Human
Rat
B.
rSeV/dM-GFP
'BioKnife-GFP'
rSeV/dMFct14 (uPA2)-GFP
U87
U138
U251
U373
A172
9L
10 μm
Cytotoxity (%)
*P<0.01
100
90
80
70
60
50
40
30
20
10
0
U87
U138
U373
A172
9L
Human
Rat
U251
Human
rSeV/dM-GFP
'BioKnife-GFP'
'BioKnife-GFP' + PAI-I (500 μg/mL)

Figure 2.

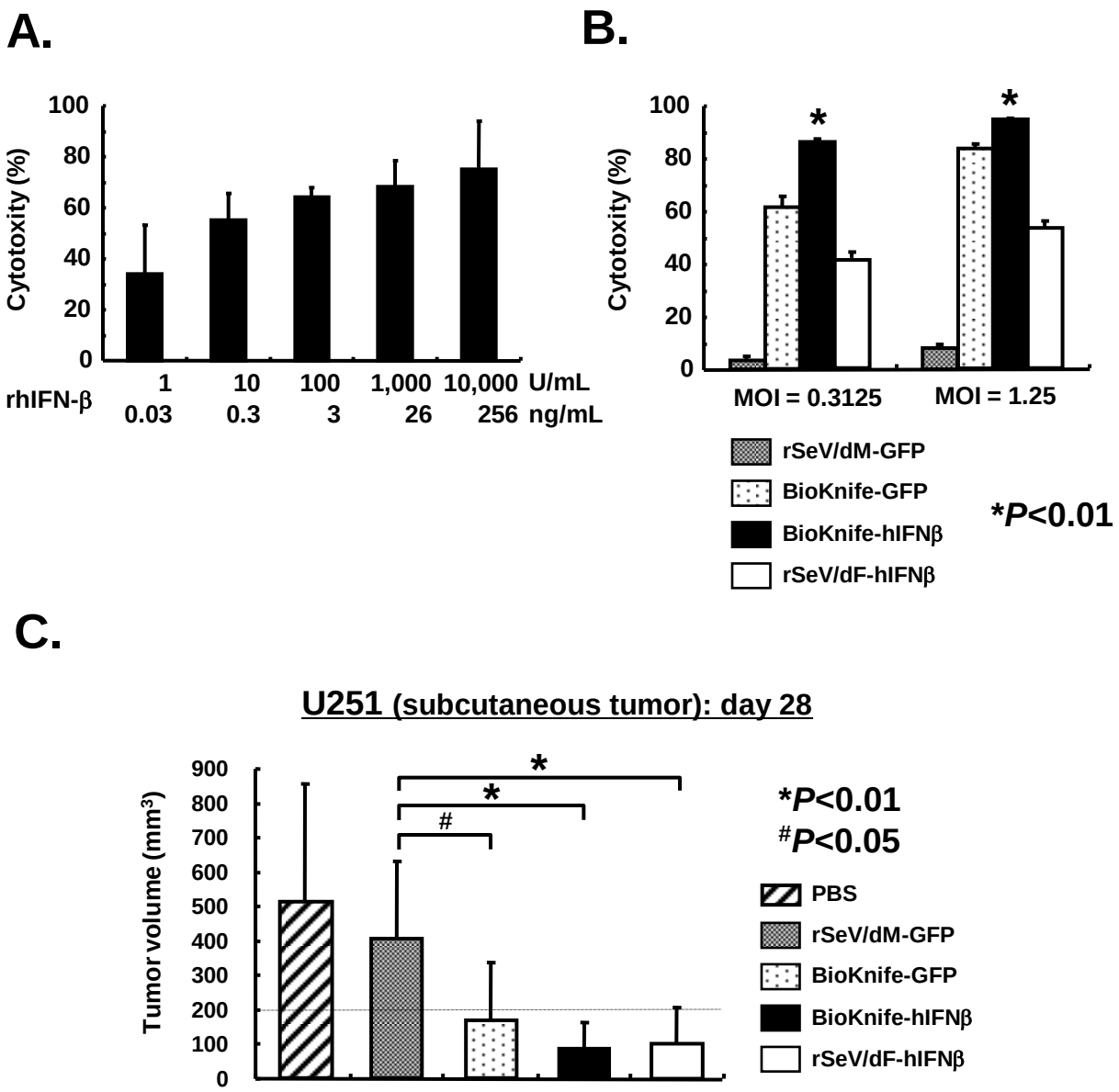
A.
B.
C.
Cytotoxity (%)
100
80
60
40
20
0
rhIFN-β
1
10
100
1,000
10,000
U/mL
0.03
0.3
3
26
256
ng/mL
MOI = 0.3125
MOI = 1.25
rSeV/dM-GFP
BioKnife-GFP
BioKnife-hIFNβ
rSeV/dF-hIFNβ
*P<0.01
U251 (subcutaneous tumor): day 28
Tumor volume (mm3)
900
800
700
600
500
400
300
200
100
0
#P<0.05
PBS

Figure 3.

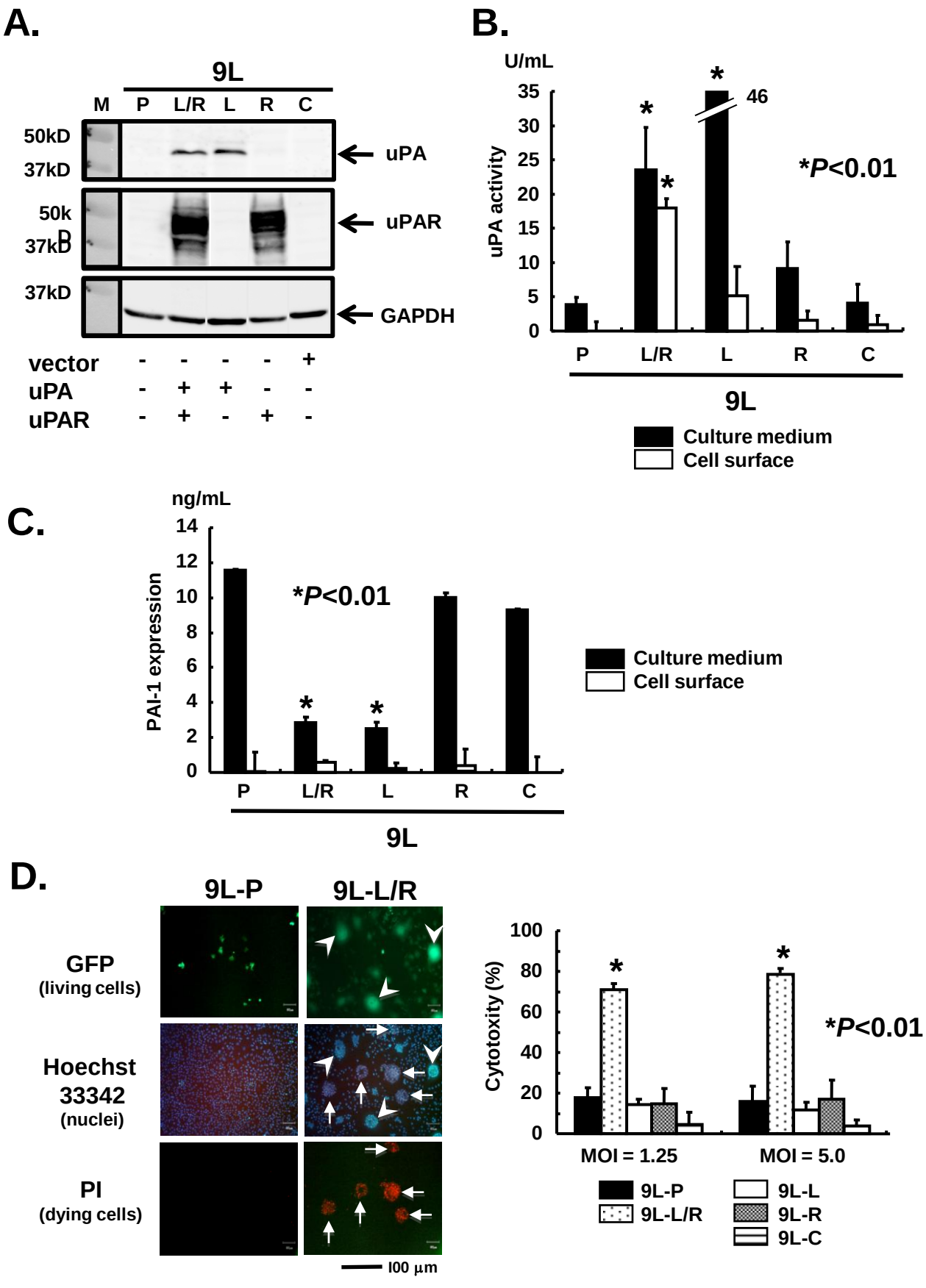
A.
9L
M
P
L/R
L
R
C
50kD
37kD
uPA
50k
37kD
uPAR
37kD
GAPDH
vector - - - - +
uPA - + + - -
uPAR - + - + -
B.
U/mL
uPA activity
35
30
25
20
15
10
5
0
46
*P<0.01
P
L/R
L
R
C
9L
Culture medium
Cell surface
C.
ng/mL
PAI-1 expression
14
12
10
8
6
4
2
0
*P<0.01
P
L/R
L
R
C
9L
Culture medium
Cell surface
D.
9L-P
9L-L/R
GFP
(living cells)
Hoechst
33342
(nuclei)
PI
(dying cells)
100 μm
Cytotoxity (%)
100
80
60
40
20
0
*P<0.01
MOI = 1.25
MOI = 5.0
9L-P
9L-L/R
9L-L
9L-R
9L-C

Figure 4.

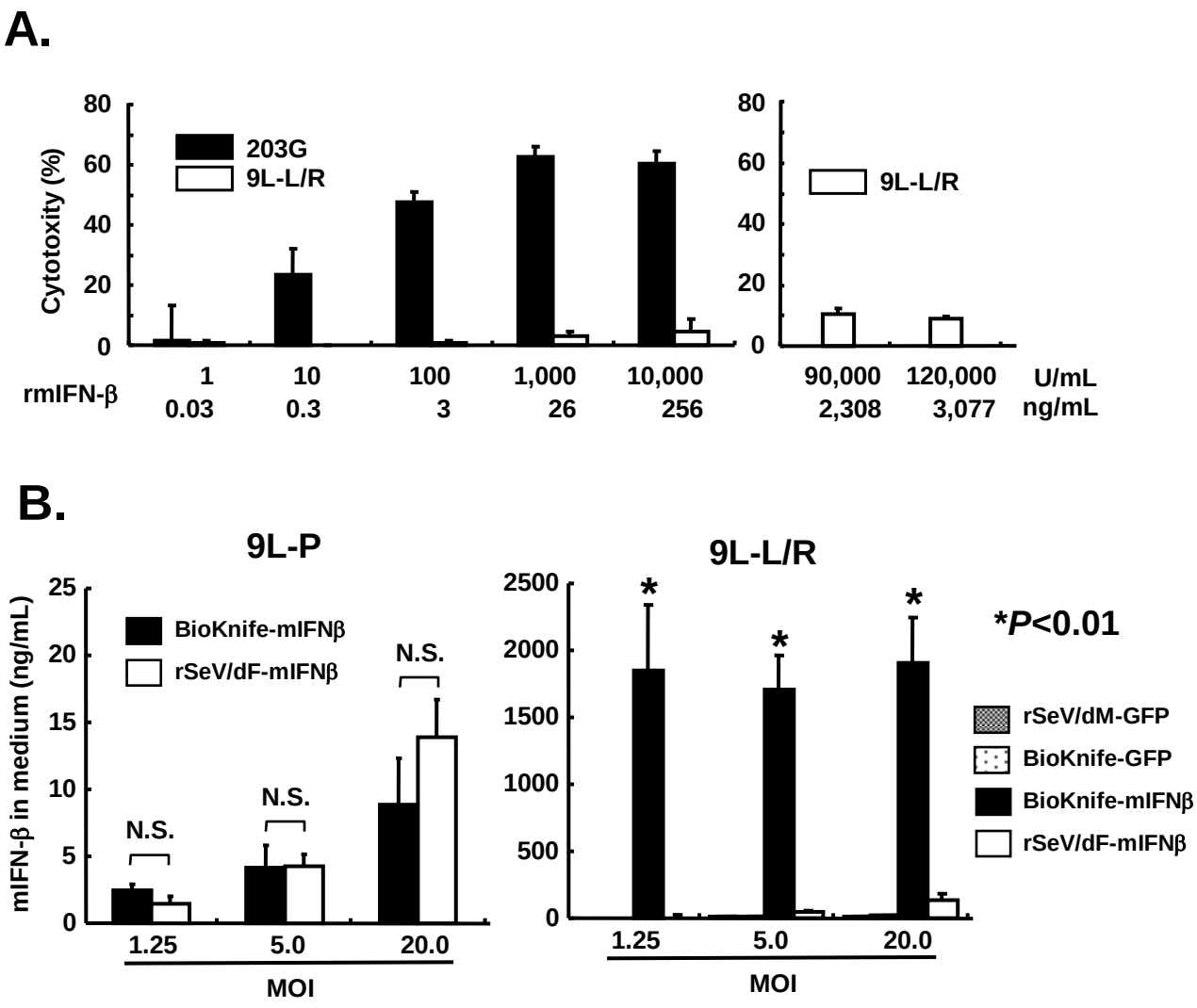
A.
Cytotoxity (%)
203G
9L-L/R
9L-L/R
rmIFN-β
1
0.03
10
0.3
100
3
1,000
26
10,000
256
90,000
2,308
120,000
3,077
U/mL
ng/mL
B.
9L-P
9L-L/R
mIFN-β in medium (ng/mL)
BioKnife-mIFNβ
rSeV/dF-mIFNβ
N.S.
N.S.
N.S.
*P<0.01
rSeV/dM-GFP
BioKnife-GFP
BioKnife-mIFNβ
rSeV/dF-mIFNβ
1.25
5.0
20.0
MOI

Figure 4. (continued)

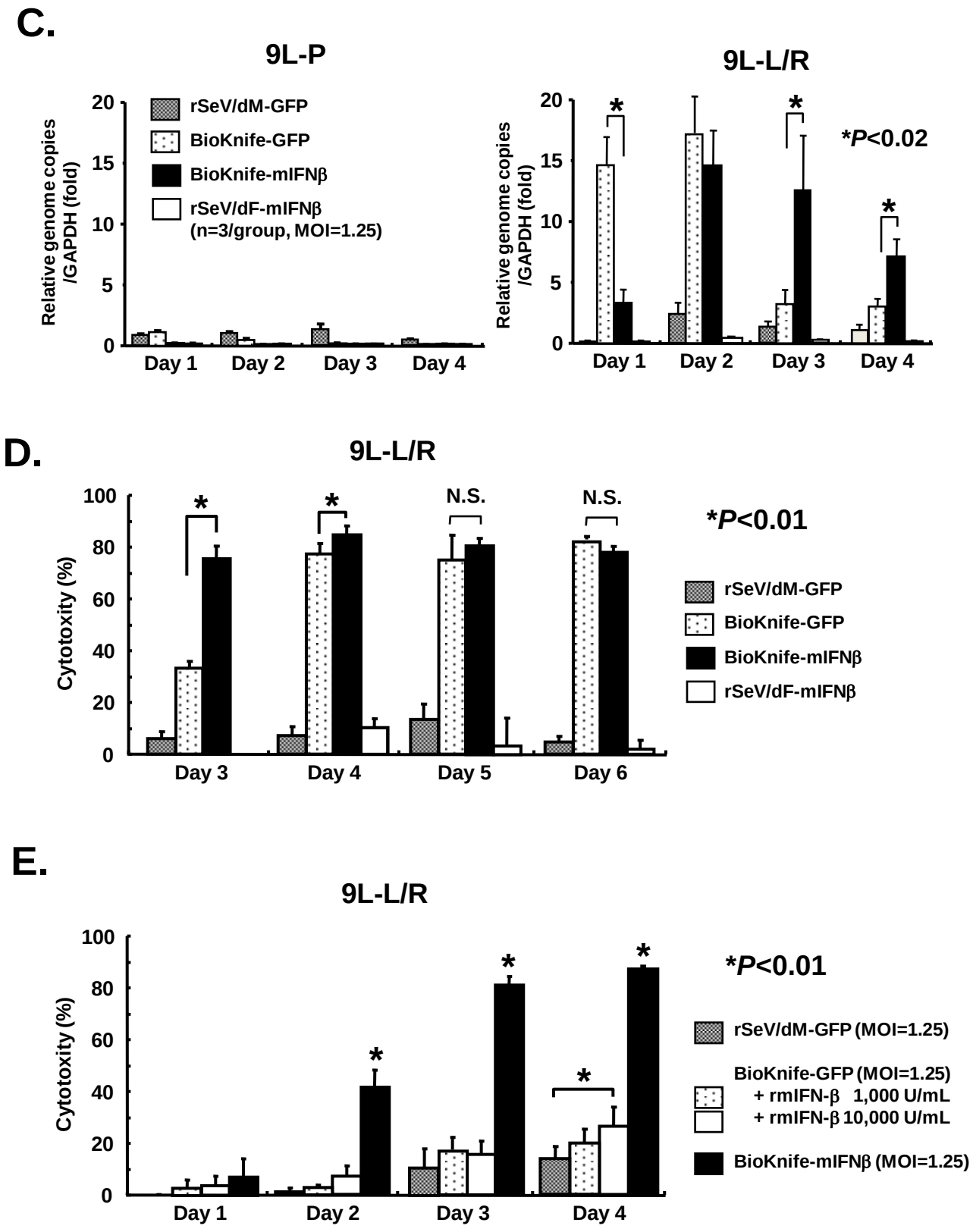

Figure 5.

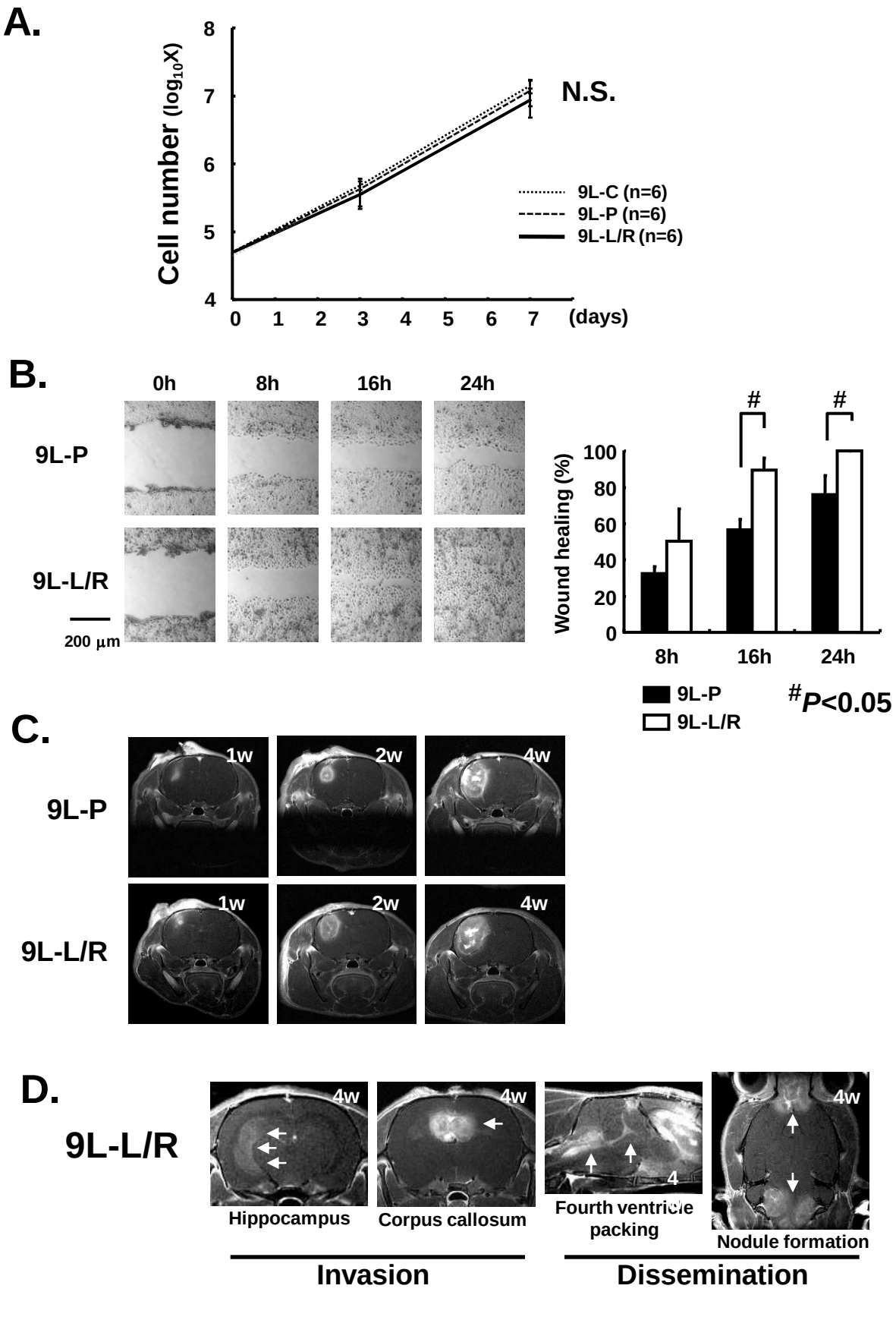
A.
Cell number (log_{10}X)
8
7
6
5
4
0 1 2 3 4 5 6 7
(days)
N.S.
9L-C (n=6)
9L-P (n=6)
9L-L/R (n=6)
B.
0h
8h
16h
24h
9L-P
9L-L/R
200 μm
Wound healing (%)
100
80
60
40
20
0
#
#
8h
16h
24h
9L-P
9L-L/R
#P<0.05
C.
9L-P
9L-L/R
1w
2w
4w
1w
2w
4w
D.
9L-L/R
4w
4w
4
4w
Hippocampus
Corpus callosum
Fourth ventricle packing
Nodule formation
Invasion
Dissemination

Figure 6.

A.

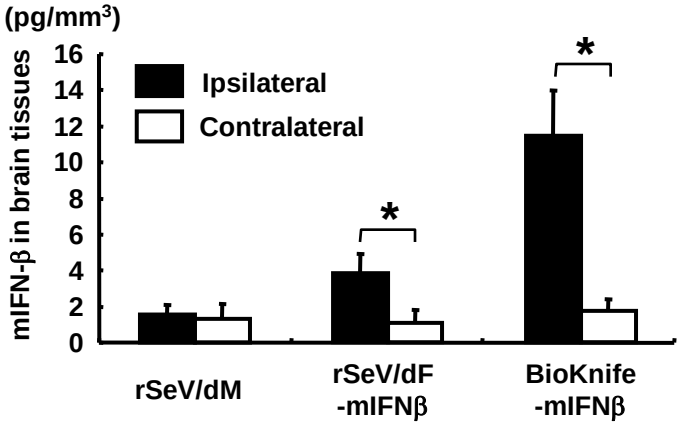

*P<0.01

B.

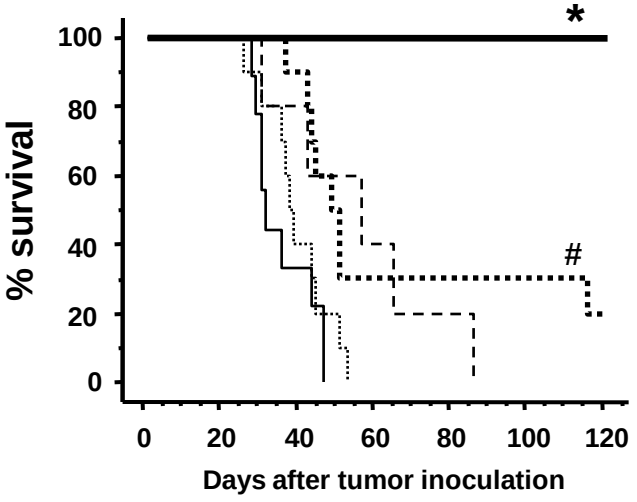

*P<0.01 vs others

#P<0.05 vs others

BioKnife-mIFNβ (n=6)

BioKnife-GFP (n=10)

rSeV/dF-mIFNβ (n=6)

rSeV/dM-GFP (n=10)

PBS (n=9)

Supplementary Figure S1.

A.

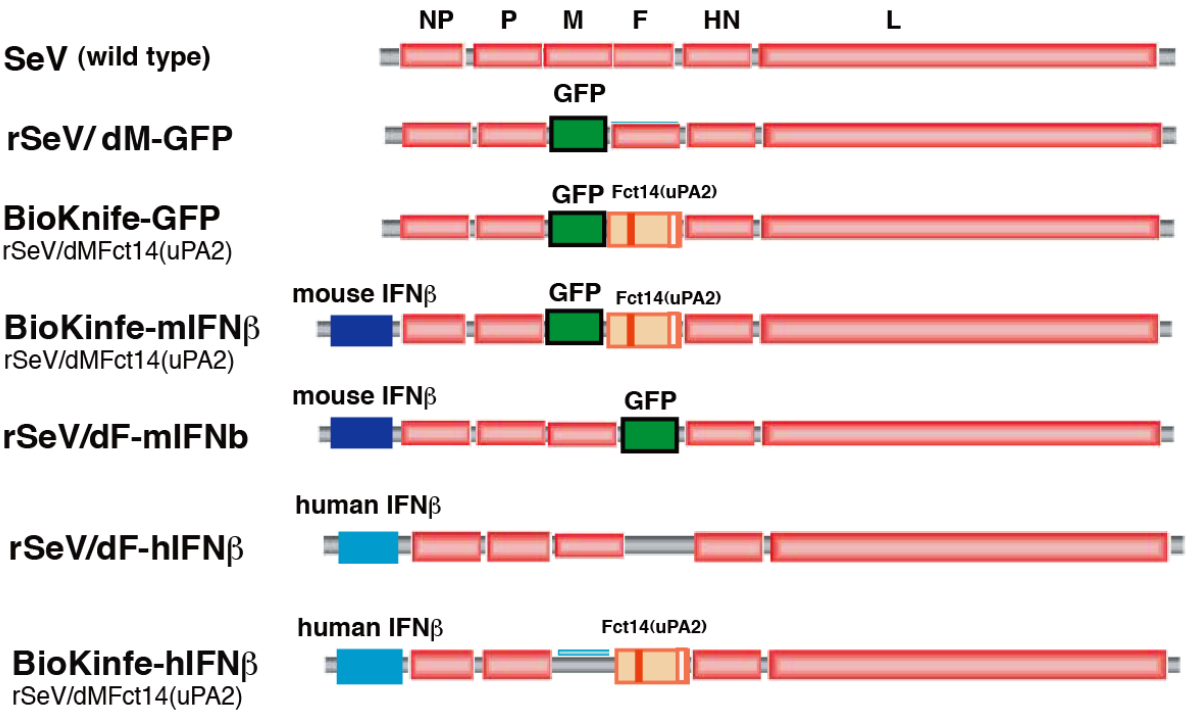

B.

Modification of cleavage site

	F2							F1				
wild type	A	G	V	P	Q	S	R	F	F	G	A	V
uPA2	A	G	V	S	G	R		S	F	F	G	A	V

Truncation of Cytoplasmic tail

	transmembrane	cytoplasmic domain
F (wild type)	VITIIVVMVVILVVIIVIIIVLY	RLKRSMLMGNPDDRIPRDTYTLEPKIRHMYTKGGFDAMAEKR
Fct14	VITIIVVMVVILVVIIVIIIVLY	RLKRSMLMGNPDDR

Supplementary Figure S2.